

## Structural and Thermoelectric Properties of AgSbSe<sub>2</sub> and AgSbTe<sub>2</sub>

K. Wojciechowski<sup>1</sup>, J. Tobola<sup>2</sup>, M. Schmidt<sup>1</sup>, R. Zybala<sup>1</sup>

<sup>1</sup> Faculty of Materials Science and Ceramics

<sup>2</sup> Faculty of Physics and Applied Computer Science

AGH University of Science and Technology, Al. Mickiewicza 30, 30-059 Cracow, Poland

e-mail : [gcwojcie@cyf-kr.edu.pl](mailto:gcwojcie@cyf-kr.edu.pl), phone: (+48)12-617-34-42

### Abstract

Undoped AgSbSe<sub>2</sub> and AgSbTe<sub>2</sub> materials were synthesized by direct fusion technique. The structural properties were investigated by X-ray diffraction and SEM microscopy. The electrical conductivity, thermal conductivity and Seebeck coefficient have been measured as a function of temperature in the range from 300 to 600 K.

To enlighten electron transport behaviors observed in AgSbSe<sub>2</sub> and AgSbTe<sub>2</sub> compounds, electronic structure calculations have been performed by the Korringa-Kohn-Rostoker method with coherent potential approximation (KKR-CPA). The calculated density of states in fully disordered cases shows apparent tendencies to opening the energy gap near the Fermi level for the stoichiometric Ag<sub>0.5</sub>Sb<sub>0.5</sub>X compositions, which well agrees with the semimetallic properties of the analyzed samples.

### Introduction

**The ternary chalcogenides AgSbSe<sub>2</sub> and AgSbTe<sub>2</sub> belongs to family of semiconductors with disordered NaCl cubic structure (s.g. Fm3m), in which silver and antimony occupy metal sublattice[1]. Both compounds are very interesting due to their thermoelectric properties (see**

Table 1), especially very low thermal conductivity  $\lambda < 1 \text{ Wm}^{-1}\text{K}^{-1}$ , which is a consequence of their disordered structure.

Table 1 Selected physical properties of AgSbSe<sub>2</sub> and AgSbTe<sub>2</sub>.

Parameter	AgSbTe <sub>2</sub>	AgSbSe <sub>2</sub>
Space group	Fm3m	Fm3m
Cell size [Å]	6.078 [1]	5.786 [1]
Density [g·cm <sup>-3</sup> ]	7.12 [1]	6.60 [1]
Band gap [eV]	0.71 <sup>b</sup> [5] 1.65 <sup>c</sup> [5]	0.091 <sup>a</sup> [8] 0.34 <sup>b</sup> [7] 1.03 <sup>c</sup> [6]
Thermal conductivity [W·m <sup>-1</sup> ·K <sup>-1</sup> ]	0.64 [3]	0.82
Electrical conductivity [S·cm <sup>-1</sup> ]	130-150 [3]	154 [9]
Seebeck coeff. [μV·K <sup>-1</sup> ]	165-240 [3]	
Melting point [°C]	555 [2]	610 [2]

<sup>a</sup> electrical measurements; <sup>b</sup> direct gap - optical measurements;

<sup>c</sup> indirect gap - optical measurements

Cubic AgSbTe<sub>2</sub> is known as a good p-type thermoelectric material, but due to its thermodynamical instability below 360°C it slowly decomposes on secondary phases:  $\alpha\text{Ag}_2\text{Te}$  and  $\text{Sb}_2\text{Te}_3$  [3], and limits its practical application. It is expected that alloying of AgSbTe<sub>2</sub> with other cubic compounds, such us: GeTe (TAGS), PbTe and SnTe, can allow stabilizing the NaCl structure.

However these alloys are also known to be complicated by their inhomogeneity, despite reports of complete solid solutions in phase diagram determinations [4]. Exceptionally high thermoelectric figure of merit  $ZT=2$ , has been reported for  $(\text{Ag}_{1-y}\text{SbTe}_2)_{0.05}(\text{PbTe})_{0.95}$ , which may involve the

nanoscale microstructure. Although, conflicting reports on the same materials claim only  $ZT$  of 1 or less. Chen et al. [4] shown that these materials are multiphase on the scale of millimeters despite appearing homogeneous by X-ray diffraction and routine electron microscopy. Using a scanning Seebeck microprobe, authors found significant variation of Seebeck coefficient including both n-type and p-type behavior in the same sample. It can not be excluded that complicated behavior of the alloys can be result of the complex nature of their parent compounds.

Despite that AgSbSe<sub>2</sub> and AgSbTe<sub>2</sub> based materials are widely investigated, the basic information about properties of pure compounds, e.g the nature of the disorder, or electronic structure are still not quite clear.

### Experimental details

The starting materials were prepared by direct fusion of stoichiometric amounts of their constituent elements (Ag, Sb, Se, Te) of purity 99.99% in sealed, evacuated silica tubes covered inside with thin layer of pyrolytical carbon. Tubes were heated in temperature controlled, cradled furnace at 700°C for 1 h, with continuous swinging to complete mixing and reaction. Tubes were gradually cooled to room temperature to obtain polycrystalline ingots. The materials were ground and hot-pressed in graphite dies (argon atmosphere,  $t = 20$  min,  $p = 30$  MPa, at  $T = 410$  °C) and slowly cooled down with rate of 1 °C/min to the room temperature in order to avoid fracturing. Because AgSbTe<sub>2</sub> can undergo decomposition below 360°C some of AgSbTe<sub>2</sub> samples were heated in evacuated quartz ampoules to 450°C and rapidly cooled down by quenching in water, in order to obtain single-phased materials. The samples of 10 mm in diameter and about 20 mm in height, were cut with a diamond saw and polished.

The prepared materials were characterized by X-ray diffractometry (X'Peret Philips system, with filtered  $\text{CuK}_\alpha$  radiation) and scanning electron microscopy (JEOL JSM-840 with an electron-probe microanalysis apparatus (EPMA). The lattice parameters were calculated from the experimental X-ray patterns using *FullProf* refinement program implementing Rietveld method. The electrical and thermal transport properties were measured over the temperature range from 300 to 600K. The electrical conductivity was determined by four-probe AC technique. The Seebeck coefficient and thermal conductivity measurements were conducted in radiation-shielded vacuum probe by forcing variable heat flux across the sample and measuring corresponding linear variations of temperature differences and thermoelectric voltage in steady-state conditions. Heat flux, passing by the cold side of the sample, was measured by previously calibrated heat-flux sensor. The results were used for precise calculations of increased heat losses due to very low thermal conductivity of measured

samples. The Hall coefficient  $R_H$  was measured using low frequency (7 Hz) AC sample current of 50 to 100 mA/mm<sup>2</sup> in a constant magnetic field of 0.705 T at the room temperature. Carrier concentrations were evaluated from the Hall coefficient  $R_H$ , assuming a Hall scattering factor equal to 1.0.

### Structural analysis

SEM observations with simultaneous EPMA analysis of the samples revealed that the resulting materials had a uniform microstructure and chemical composition. The AgSbTe<sub>2</sub> samples contained well-formed grains with sizes ranging from 5 to 50 μm. However, all AgSbTe<sub>2</sub> samples had visible Widmanstätten-like texture. It has been suggested in [10] that the pattern is associated with the presence of Sb<sub>2</sub>Te<sub>3</sub> as a Widmanstätten precipitate along {111} planes in the AgSbTe<sub>2</sub>. Conversely, AgSbSe<sub>2</sub> samples had a glass-like texture without visible grain borders. XRD analysis of AgSbSe<sub>2</sub> and fast cooled AgSbTe<sub>2</sub> samples shows that obtained materials were single-phased. In case of slowly cooled samples of AgSbTe<sub>2</sub> small amount (<10%) of other phases were noticed. The measured densities of all materials were found to be at least 98% of their crystallographic densities.

The Rietveld refinement method was used for refining structure parameters for the model of the disordered NaCl structure ( $Fm\bar{3}m$ ) and various models of ordered ABX<sub>2</sub> - type structures. There were considered the most common superstructures of NaCl: e.g.  $\alpha$ -NaFeO<sub>2</sub> ( $R\bar{3}m$ ), LiTbS<sub>2</sub> ( $Fd\bar{3}m$ ) and  $\gamma$ -LiFeO<sub>2</sub> ( $I4_1/amd$ ). Analysis of "goodness of fit" statistical parameters for the refinement results, such as:  $\chi^2$ ,  $R_{wp}$ , and Durbin-Watson statistics, show that all the models describe experimental data practically with the same precision and therefore they are very similar within these criteria. Moreover, in all calculated diffraction patterns, intensities of characteristic superstructure reflections are lower than the experimental background signal. These results are a consequence of very similar X-ray scattering factors of Ag and Sb for CuK $\alpha$  radiation ( $f_{Ag}=47.2+4.3i$  and  $f_{Sb}=50.9+5.7i$  respectively). Therefore, it seems that the nature of ordering in the AgSbSe<sub>2</sub> and AgSbTe<sub>2</sub> structure can not be easily investigated by classical X-ray diffraction techniques. However, preliminary structural calculations show that such analysis would be possible e.g. by using neutron radiation (CW or TOF method).

### Transport properties

Studies of temperature dependences of electrical conductivity revealed that AgSbSe<sub>2</sub> and AgSbTe<sub>2</sub> exhibit semimetallic/semiconducting behavior. The activation energies  $E_a$  for both compounds, determined using an Arrhenius law, are about 0.03 eV and remain close to another result of 0.09 eV obtained from electrical investigations (see

Table 1). On the other hand, these data are much lower than values of direct band gap energy  $E_g^d$  (0.3 to 0.71 eV) measured by optical method for intrinsic absorption region. It may suggest that results of electrical investigations correspond rather to activation energy of extrinsic charge carriers, but another explanation of discrepancies may lay in significant differences in microstructure of samples (thin layer vs. bulk polycrystalline material).

The magnitude of the Seebeck coefficient of AgSbTe<sub>2</sub> at the room temperature is consistent with semimetallic behavior of this sample ( $\alpha=68 \mu\text{VK}^{-1}$ ). The Seebeck coefficient for AgSbSe<sub>2</sub> is larger (320  $\mu\text{VK}^{-1}$ ) what can be a symptom of more semiconducting character of this compound.

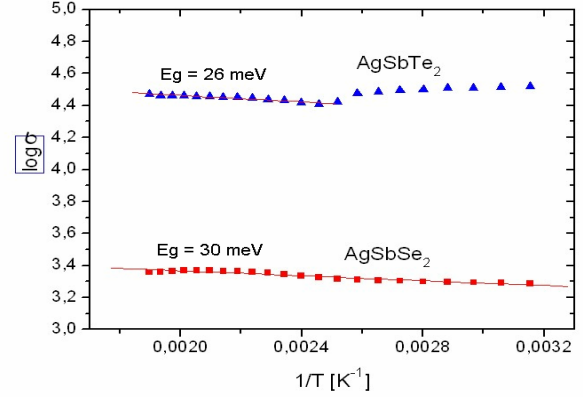


Fig. 1 Temperature dependence of electrical conductivity of AgSbSe<sub>2</sub> and AgSbTe<sub>2</sub>.

Both materials exhibit *p*-type of conductivity and relatively large Hall concentration of carriers of  $1 \cdot 10^{19} \text{ cm}^{-3}$  and  $5 \cdot 10^{19} \text{ cm}^{-3}$  for AgSbSe<sub>2</sub> and AgSbTe<sub>2</sub> respectively. The Seebeck coefficient and Hall carrier concentration data were used to estimation of effective mass of carriers  $m^*$ , assuming a single parabolic band model with acoustic phonon scattering as a predominant carrier scattering mechanism.

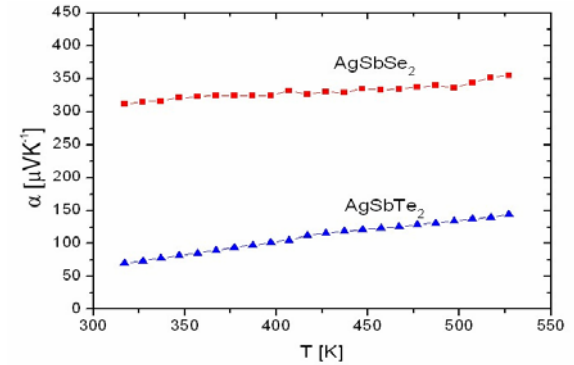


Fig. 2 Temperature dependence of the Seebeck coefficient values of AgSbSe<sub>2</sub> and AgSbTe<sub>2</sub>.

Calculated effective masses of carriers are significantly different:  $m^* = 2.7$  for AgSbTe<sub>2</sub> and 0.7 for AgSbSe<sub>2</sub>, despite of comparable mobilities ( $40 \div 50 \text{ cm}^2 \text{ s}^{-1} \text{ V}^{-1}$ ). Dissimilar effective masses  $m^*$  can indicated on differences in band structure of both compounds near the Fermi energy.

Table 2. Thermoelectric properties of undoped AgSbTe<sub>2</sub> and AgSbSe<sub>2</sub> samples at room temperature.

Parameter	AgSbTe <sub>2</sub>	AgSbSe <sub>2</sub>
Cell size $a$ [Å]	6.0816	5.7883
Band gap $E_g$ [meV]	26	30
Electrical conductivity $\sigma$ [ $\text{S} \cdot \text{cm}^{-1}$ ]	332	79
Seebeck coeff. [ $\mu\text{V} \cdot \text{K}^{-1}$ ]	68	320
Thermal conductivity $\lambda$ [ $\text{W} \cdot \text{m}^{-1} \cdot \text{K}^{-1}$ ]	1.15	0.81
Elec. cont. of therm. condct. $\lambda_{el}$ [ $\text{W} \cdot \text{m}^{-1} \cdot \text{K}^{-1}$ ]	0.2	0.04
Type of majority carriers	<i>p</i>	<i>p</i>
Hall carrier concentration $n$ [ $\text{cm}^{-3}$ ]	$5.0 \cdot 10^{19}$	$1.0 \cdot 10^{19}$
Hall mobility $\mu$ [ $\text{cm}^2 \text{ s}^{-1} \text{ V}^{-1}$ ]	41	49.2
Carrier effective mass $m^*/m_0$	2.7	0.7

The samples of  $\text{AgSbSe}_2$  and  $\text{AgSbTe}_2$  demonstrate very low thermal conductivity (see Table 2). The measured value for  $\text{AgSbSe}_2$  at room temperature is in excellent agreement with literature data (Table 1). Thermal conductivity of  $\text{AgSbTe}_2$  is higher than earlier reported value ( $0.6\text{W}\cdot\text{m}^{-1}\text{K}^{-1}$ ). The discrepancy can be result of different amount of secondary phase inclusions and larger electrical conductivity. Calculated, on basis of Wiedemann-Franz-Lorenz law, electronic contribution of thermal conductivity  $\lambda_{el}$  equals about 18% of the total thermal conductivity  $\lambda$ .

### Electronic structure

Electronic structure computations on ordered and disordered  $\text{AgSbSe}_2$  and  $\text{AgSbTe}_2$  alloys as well as their hypothetical NaCl-type parent compounds have been performed using KKR method [15,16]. The coherent potential approximation (CPA) has also been incorporated to account for chemically disordered materials. The crystal potential of muffin-tin form has been constructed within the LDA framework, using von Barth-Hedin parametrization for the exchange-correlation part. For well-converged charge and potentials, the total, site-decomposed and  $l$ -decomposed density of states (DOS) were computed applying k-space tetrahedron integration. The Fermi level was determined from the generalised Lloyd formula.

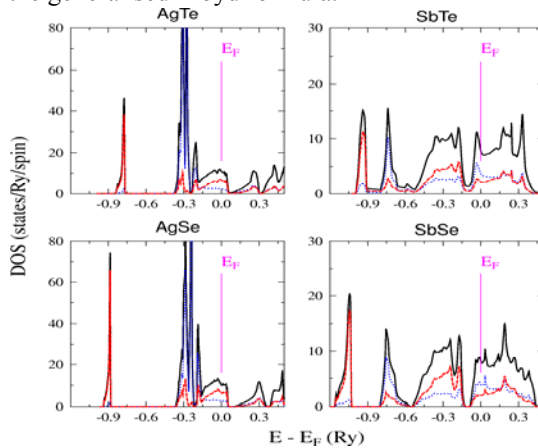


**Fig. 3** DOS of hypothetical NaCl-type parent compounds  $\text{AgSe}$ ,  $\text{AgTe}$ ,  $\text{SbSe}$  and  $\text{SbTe}$ . Black (solid), blue (dot) and red (dash) lines represent total, 'left' (Ag, Sb) and 'right' (Se, Te) DOS, respectively.

The electronic properties of fully disordered system within the NaCl-type structure, corresponding to the chemical formula  $\text{Ag}_{0.5}\text{Sb}_{0.5}\text{X}$  ( $\text{X} = \text{Se}$  and  $\text{Te}$ ), have been compared to results of computations for ordered crystal structures. In order to better enlighten the origin of ground state properties of  $\text{AgSbSe}_2$  and  $\text{AgSbTe}_2$  systems, electronic structure has been also studied in hypothetical end-point binary compounds  $\text{AgX}$  and  $\text{SbX}$ . Moreover, the electronic structure of chemically ordered binary and ternary systems was computed by the KKR as well as the FLAPW techniques. In the calculations of all selenides and tellurides we used the experimental values of lattice constants determined in  $\text{AgSbSe}_2$  and  $\text{AgSbTe}_2$ , respectively.

#### Binary compounds $\text{AgX}$ and $\text{SbX}$

The investigations of DOS characteristics in hypothetical  $\text{AgX}$  and  $\text{SbX}$  allow to better understand complexity of forming semimetallic properties in  $\text{AgSbX}_2$ . Fig. 3 shows

that all these binary compounds have metallic ground states, but with different position of the Fermi level ( $E_F$ ) with respect to the low valley (or a true energy gap) appearing on DOS.

Band structure of  $\text{AgX}$  consists of lower lying  $s$ -like states, coming essentially from  $X$  atom, and the block of presumably  $d$ -Ag and  $p$ -X states, enabling to accommodate 16 electrons. The semiconducting properties would be expected if all these bands are completely filled. Since  $\text{AgX}$  possess 17 valence electrons, the Fermi level  $E_F$  is placed in upper region of the valence bands. Consequently,  $\text{AgX}$  (VEC=17) can be viewed as one-hole compounds, since one electron must be added to reach the deep DOS valley. Electronic structure of  $\text{SbX}$  consists of four successive blocks of bands. The lower lying two separate and narrow  $s$ -DOS peaks arrive from  $X$  and Sb atoms. The higher lying two blocks of strongly hybridised  $p$ -states from  $X$  and Sb, are separated by a true gap or a deep DOS minimum seen in  $\text{SbSe}$  and  $\text{SbTe}$ , respectively. The semiconducting properties would be expected for VEC=8. Consequently, the  $\text{SbX}$  (VEC=9) systems can be viewed as a one-electron compounds due to the Fermi falling at the bottom of the conduction band. From the analysis of hypothetical binary parent compounds, we see that there is a subtle difference between selenides and tellurides due to the presence of the energy gap between valence and conduction bands in  $\text{AgSe}$  and  $\text{SbSe}$ , whereas only a deep DOS minimum in  $\text{AgTe}$  and  $\text{SbTe}$ .

#### Ternary ordered $\text{AgSbX}_2$

Our computations of different crystallographically ordered approximants of  $\text{AgSbX}_2$  (resulting in the X-ray diffraction patterns similar to that received for disordered NaCl-type structure, see Table 3) show that their ground state electronic properties are really close. In all considered cases, the Fermi level is found either in the deep valley (semimetallic) or in the true energy gap (semiconducting) depending on different atomic arrangements.

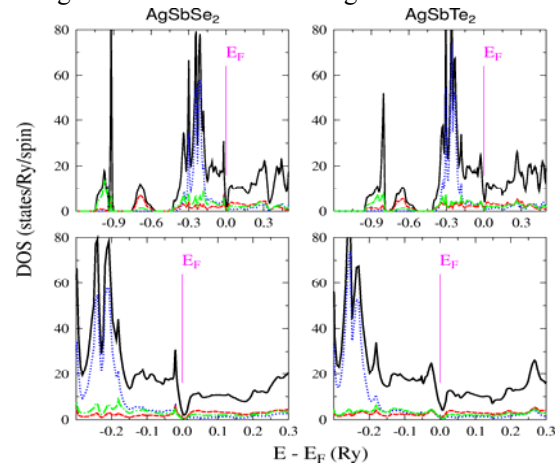


**Fig. 4** DOS of ordered approximant of  $\text{AgSbX}_2$ . Black (solid), blue (dot), red (dash), green (dot-dash) lines represent total, Ag, Sb and X contributions, respectively. Bottom – enlarged DOS near  $E_F$ .

#### Fully disordered $\text{Ag}_{0.5}\text{Sb}_{0.5}\text{X}$

The appearance of semimetallic (semiconducting) properties in NaCl-type disordered  $\text{AgSbX}_2$  is not so evident from the analysis of binary parent compounds, since the Fermi level was expected to fall into the gap at VEC=8 or

VEC=18, but antimony possesses four electrons more than silver.

**Table 3 Results of computations for the disordered structure (Fm3m) and selected possible ordered systems of AgSbSe<sub>2</sub>.**

Symbol	s.g.	$E_g$	Position of the Fermi level $E_f$
D1	Fm3m	semimetal	minimum of DOS
A1	R-3m	semimetal	valence bands
B1	Fd-3m	~0.0 eV	minimum of DOS
F1	I4 <sub>1</sub> /amd	semimetal	conduction bands
G1	Pmmn	semimetal	valence bands

Hence, the onset of pseudo-gap on DOS seems to be related to the specific hybridisation of different type of orbitals ( $d$ -orbitals of Ag and  $p$ -orbitals of Sb) in alloyed system. Indeed, the electronic structure variation of Ag<sub>1-x</sub>Sb<sub>x</sub>X (Fig. 5) can not be understood in terms of rigid band behaviour and a simple shift of  $E_F$  when the number valence electron number increases. In fact, the change in relative Ag/Sb content strongly modifies the population and hybridisation of  $d$ -type Ag and  $sp$ -type Sb orbitals. The critical number of valence electrons to establish the pseudo-gap appears for VEC=14.

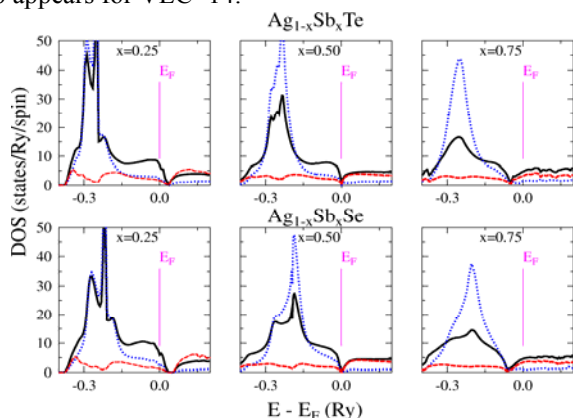


**Fig. 5 Evolution of DOS near the Fermi level in solid solutions Ag<sub>1-x</sub>Sb<sub>x</sub>X (X = Se and Te).**

Noteworthy, the evolution of DOS in both cases shows subtle differences, since in tellurides have slightly higher DOS value at  $E_F$  than in the values in selenides, which remains in line with electronic properties detected in binary (true energy gap in selenides against a deep valley in tellurides). Inspecting DOS characteristics of disordered Ag<sub>0.5</sub>Sb<sub>0.5</sub>X (Fig. 4) leads to the conclusion that the variation of valence-like DOS is stronger than the corresponding one of the conduction-like DOS. This result well supports the experimental finding revealing larger absolute thermopower in  $p$ -type AgSbX<sub>2</sub> materials than in  $n$ -type samples.

## Conclusions

Experimental studies of AgSbSe<sub>2</sub> and AgSbTe<sub>2</sub> show that both compounds are  $p$ -type semimetals or very narrow-gap semiconductors ( $E_g = 0.03$  eV). The Seebeck coefficient of AgSbTe<sub>2</sub> at the room temperature ( $\alpha = 68 \mu\text{VK}^{-1}$ ) confirms its semimetallic properties; whereas AgSbSe<sub>2</sub> seems to be more semiconducting ( $\alpha = 320 \mu\text{VK}^{-1}$ ).

The electronic structure calculations well support experimental results. DOS computations in fully disordered

as well as in different ordered approximants of AgSbX<sub>2</sub> show that in most cases their ground state properties are semimetallic due to slight overlapping of conduction and valence bands near the Fermi energy. Moreover, the larger value of Seebeck coefficient for AgSbSe<sub>2</sub>, in comparison to AgSbTe<sub>2</sub>, can be related to relatively stronger variation of valence-like DOS as well as lower  $n(E_f)$  in the former.

Besides, we suggest that the presence of low DOS near  $E_f$  in AgSbX<sub>2</sub> allows easily tuning the Seebeck coefficient sign upon suitable doping/substitution. However,  $n$ -type AgSbX<sub>2</sub> compounds are expected to have smaller thermopower than the presented here  $p$ -type materials, as can be roughly detected on the KKR-CPA DOS.

## Acknowledgments

The work was supported by The EEA Financial Mechanism & The Norwegian Financial Mechanism, (grant No PL0089-SGE-00104-E-V2-EEA, 2007-2010)

## References

- [1]. Geller S. *et al*, „Ternary Semiconducting Compounds with Sodium Chloride-Like Structure: AgSbSe<sub>2</sub>, AgSbTe<sub>2</sub>, AgBiS<sub>2</sub>, AgBiSe<sub>2</sub>”. *Acta Cryst.* Vol. 12 (1959), pp. 46.
- [2]. Wernick J.H. *et al*, semiconducting ternary compounds”, *Phys. Soc.* Vol. 21, 1957
- [3]. Wolfe R. *et al*, Anomalous Hall Effect in AgSbTe<sub>2</sub>, *J. Appl. Phys.*, Vol. 31, 1960, pp. 1959-1964
- [4]. Chen N. *et al*, “Macroscopic thermoelectric inhomogeneities in (AgSbTe<sub>2</sub>)<sub>x</sub>(PbTe)<sub>1-x</sub>” *Appl. Phys. Lett.* Vol. 87, 2005, pp.171903
- [5]. Zayed H.A. *et al*, “Optical absorption behavior of AgSbTe<sub>2</sub> thin films” *Vacuum.* Vol. 47, No. 1, 1996, pp. 49-51
- [6]. Soliman H. S. *et al*, “Optical properties of thermally vacuum evaporated AgSbSe<sub>2</sub> thin films” *J. Phys.: Condens. Matter* Vol.10, 1998, pp. 847-856
- [7]. Abdelghany A. *et al*,: Electrical conductivity and thermoelectric power of AgSbSe<sub>2</sub> “ *Mat. Chem. and Phys.* Vol. 44, 1996, pp.277-280
- [8]. Patel A. R. *et al*, “Growth and Crystallization of AgSbSe<sub>2</sub> Films”. *Thin Solids Films*, Vol 98, 1982, pp.51-57
- [9]. Kumar R.S. *et al*, “Synthesis and high pressure studies of the semiconductor AgSbSe<sub>2</sub>” *J Alloys and Compnd.* 285, 1999, pp.48-50
- [10]. Armstrong R. *et al*, A Structural Study of the compound AgSbTe<sub>2</sub> *J. Appl. Phys.* 31, 1960, 1954
- [11]. Bansil A. *et al*, “Electronic structure and magnetism of Fe<sub>3-x</sub>V<sub>x</sub>X (X=Si, Ga, and Al) alloys by the KKR-CPA method” *Phys. Rev. B* 60, 1999, pp.13396
- [12]. Wojciechowski K.T. *et al*, “Thermoelectric properties and electronic structure of CoSb<sub>3</sub> doped with Se and Te”, *J. Alloys Compd.* Vol. 361 2003, pp.19.